Chinese Chemical Letters 37 (2026) 110710

Contents lists available at ScienceDirect

Chinese Chemical Letters

journal homepage: www.elsevier.com/locate/cclet

Construction of through-space charge transfer donor-acceptor coordination polymers through the combination of planar electron-deficient/rich ligands

Zhen-Wei Zhang[a,d,1], Da-Shuai Zhang[a,d,1,*], Wei Wang[a,d], Xiao-Ting Liu[c], Hui Hu[a], Yong-Zheng Zhang[a], Longlong Geng[a,d], Bin Li[a], Yuchen Deng[a], Rongmin Wei[a], Xiuling Zhang[a,d], Yuexing Zhang[a,*], Ze Chang[b,*]

[a] *Shandong Provincial Key Laboratory of Monocrystalline Silicon Semiconductor Materials and Technology, Shandong Universities Engineering Research Center of Integrated Circuits Functional Materials and Expanded Applications, College of Chemistry and Chemical Engineering, Dezhou University, Dezhou 253023, China*

[b] *School of Materials Science and Engineering, Nankai University, Tianjin 300350, China*

[c] *College of Chemistry, Zhengzhou University, Zhengzhou 450001, China*

[d] *School of Chemistry and Chemical Engineering, Shandong University of Technology, Zibo 255000, China*

ARTICLE INFO

Article history:
Received 13 October 2024
Revised 25 November 2024
Accepted 3 December 2024
Available online 31 January 2025

Keywords:
Donor-acceptor
Coordination polymers
Through-space charge transfer
Tunable luminescence
Temperature sensing

ABSTRACT

In this paper, a new series of donor-acceptor coordination polymers (DACPs), $[Cd(dppz)(R\text{-}ndc)(H_2O)]_n$ (R = none, DZU-400; R = F, DZU-400-F; R = Br, DZU-400-Br; DZU is short for Dezhou University), $[Cd(dppz)(adc)(H_2O)]_n$ (DZU-401), and $\{[Cd(dppz)(adb)_{0.5}(HCOO)(H_2O)]\}_n$ (DZU-402), have been successfully constructed through the combination of electron-deficient dipyrido[3,2-a:2′,3′-c]phenazine (dppz) as an acceptor and various dicarboxylic ligands (H_2ndc = 2,3-naphthalenedicarboxylic acid, F-H_2ndc = 6,7-difluoronaphthalene-2,3-dicarboxylic acid, Br-H_2ndc = 6,7-dibromonaphthalene-2,3-dicarboxylic acid, H_2adc = 9,10-anthracenedicarboxylic acid, and H_2adb = 4,4′-(anthracene-9,10-diyl)dibenzoic acid) with electron-rich planar aromatic rings as donors. Structural analyses reveal closely parallel arrangement of the planar acceptor and donor units in these DACPs, which could facilitate the through-space charge transfer (TSCT) interactions of the D-A systems and the corresponding luminescent properties. Interestingly, the DACPs show highly regulable donor dependent photoluminescence from blue to orange. Based on the TSCT based luminescence and the high thermal stability of the DACPs, their thermal-stimuli responsive emission properties were further studied. Photoluminescence intensity of the DACPs all present good linearity with temperature (298–473 K), as proved by variable temperature fluorescence spectra. Importantly, the temperature sensing process is reversible and recyclable, suggesting the promising applications of the DACPs as thermal-stimuli responsive materials.

© 2025 Published by Elsevier B.V. on behalf of Chinese Chemical Society and Institute of Materia Medica, Chinese Academy of Medical Sciences.

The combination of organic electron donors (D) and electron acceptors (A) to form donor-acceptor (D−A) system has become an important strategy for the construction of optoelectronic functional materials [1–6]. In these materials, the photoelectric function essentially originated from the charge transfer interaction between the donor and acceptor moieties, including through-bond charge transfer (TBCT) [7] and/or through-space charge transfer (TSCT) [8]. By comparison, TSCT, due to its excellent stimulus responsiveness and adjustability, has been applied in the design of various new organic optoelectronic materials [9–12]. Despite all this, to realize the controllable assembly of organic D−A systems remains a highly challenging task, due to the influence of various synthetic factors.

In recent years, coordination polymers (CP) have become a new type of crystalline functional material with great development potential, due to their high adjustability and designability, as well as excellent performance in adsorption and separation, catalysis, luminescence, and other aspects [13–32]. By utilizing the advantages of CPs in structure and property regulation, the controllable assembly of TSCT based D−A systems with high adjustability could be realized by introducing the D−A species into CPs. For example, we have demonstrated the effectiveness of using host-guest

* Corresponding authors.
E-mail addresses: dashuai_74@163.com (D.-S. Zhang), zhangyuexing@sdu.edu.cn (Y. Zhang), changze@nankai.edu.cn (Z. Chang).
[1] These authors contributed equally to this work.

https://doi.org/10.1016/j.cclet.2024.110710
1001-8417/© 2025 Published by Elsevier B.V. on behalf of Chinese Chemical Society and Institute of Materia Medica, Chinese Academy of Medical Sciences.

CPs as platform for the rational construction and engineering of D–A materials [33–37]. In these works, 3D coordination framework (NKU-111) with electron-deficient coordination spaces has been constructed by using an electron deficient ligand 2,4,6-tri(4-pyridinyl)−1,3,5-triazine (tpt) with 1,3,5-triazine as the A moiety, and then by introducing different electron-rich guests as D components to tune the D−A interactions, TSCT interactions could be accessed through the π stacking of D–A units. Therefore, a series of TSCT based donor-acceptor coordination polymers (DACP) have been obtained with highly regulable photoluminescence. However, the incorporated guests are somewhat hard to determine by X-ray single crystal diffraction, which is unfavorable for the structure-property studies.

Considering the designability of CPs, combining ligand with electron-deficient unit (A) and ligand with electron-rich unit (D) into one coordination framework might be another effective and feasible strategy for the construction of novel D−A systems based on TSCT with ordered arrangement of D−A components [38]. First, the synergy of coordination interaction and D−A interaction could further stabilize the framework, benefiting the structural determination of the DACPs. Second, through the utilization of ligands with different kinds of D or A units, a series of TSCT based photoluminescence materials could be obtained with different photophysical properties. Third, based on the same D−A structure, the luminescence could be further accurately modulated by the ligand decoration with different functional groups. With this in mind, we present here the construction of a new series of TSCT based DACPs, $[Cd(dppz)(R\text{-}ndc)(H_2O)]_n$ (R = none, DZU-400; R = F, DZU-400-F; R = Br, DZU-400-Br), $[Cd(dppz)(adc)(H_2O)]_n$ (DZU-401), $\{[Cd(dppz)(adb)_{0.5}(HCOO)(H_2O)]\}_n$ (DZU-402), by using dipyrido[3,2-a:2′,3′-c]phenazine (dppz) as an acceptor and various dicarboxylic ligands (H_2ndc = 2,3-naphthalenedicarboxylic acid, F-H_2ndc = 6,7-difluoronaphthalene-2,3-dicarboxylic acid, Br-H_2ndc = 6,7-dibromonaphthalene-2,3-dicarboxylic acid, H_2adc = 9,10-anthracenedicarboxylic acid, H_2adb = 4,4′-(anthracene-9,10-diyl)dibenzoic acid) with planar aromatic rings as donors. In these DACPs, through the modulation of donor ligands, photoluminescence could be tuned in a wide visible light range from blue to orange. Structural analyses and theoretical studies demonstrate the TSCT based photoluminescence properties of these DACPs. Moreover, based on the high thermal stability of the DACPs, their reversible thermal-stimuli responsive properties were also studied by varied temperature fluorescence spectra, which reveal good linearity between the temperature and fluorescence intensity under high temperature range.

Generally, $Cd(NO_3)_2{\cdot}4H_2O$ (24.6 mg, 0.08 mmol), dppz (7 mg, 0.025 mmol), donor ligand (0.025 mmol) were dissolved in a mixed solution of DMF (0.75 mL), MeOH (0.5 mL) and H_2O (0.75 mL), which was placed in a 4 mL capped vial and further heated at 90 °C for 2 days. Block crystals with different colors were collected by filtration, washed with DMF and dried in air. The yield is 53 % for DZU-400 (colorless), 57 % for DZU-401 (yellow), and 55 % for DZU-402 (orange) based on dppz ligand, respectively.

Single-crystal X-ray diffraction analysis reveals that DZU-400 crystallizes in the triclinic crystal system, with a space group of *P*-1. The asymmetric unit comprises one crystallographically independent Cd^{2+} ion, one dppz ligand, one ndc^{2-} ligand, and a coordinated water molecule. As shown in Fig. 1a, Cd1 exhibits a six-coordination twisted octahedral geometric configuration, bonded with two nitrogen atoms from the dppz ligand, three carboxylic oxygen atoms from different ndc^{2-} ligands, and one water molecule. Two adjacent Cd^{2+} ions are closely connected to form a binuclear $Cd_2(COO)_2(H_2O)$ cluster through two carboxy groups (Fig. 1b). The Cd2 clusters are further linked by the ndc^{2-} ligands in a η^1 and μ_2-η^1:η^1 linkage mode, generating the 1D chain structure (Fig. 1c). Then the dppz ligands are anchored into the 1D chains through the chelating coordination with the Cd^{2+} ions, and the dppz ligands acting as electron acceptors exhibits a parallel staggered arrangement (Fig. 1d) with the naphthalene unit (donor) of ndc^{2-} ligands, showing a face-to-face distance of about 3.4 Å Finally, the 3D supramolecular structure (Fig. 1e) is formed through the packing of 1D D−A chains.

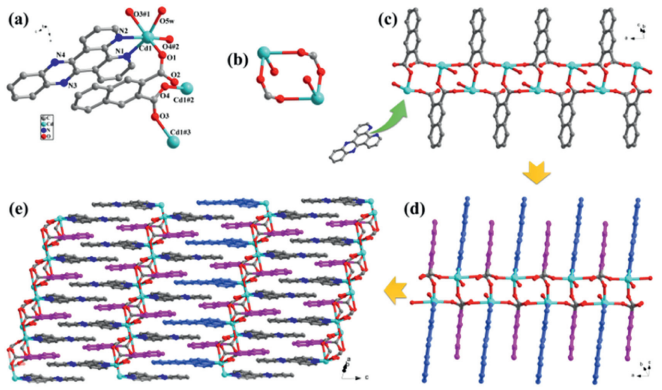


Fig. 1. Structures of DZU-400: (a) coordination environment of the Cd centers. (b) The binuclear clusters formed by two neighbouring Cd ions, two carboxylic groups and two water molecules. (c) Formation of the 1D chain structures by the connection of ndc^{2-} ligands with the Cd2 clusters. (d) Formation of the parallel staggered arrangement of the donor and acceptor in the 1D chains. (e) Packing mode of the final structures.

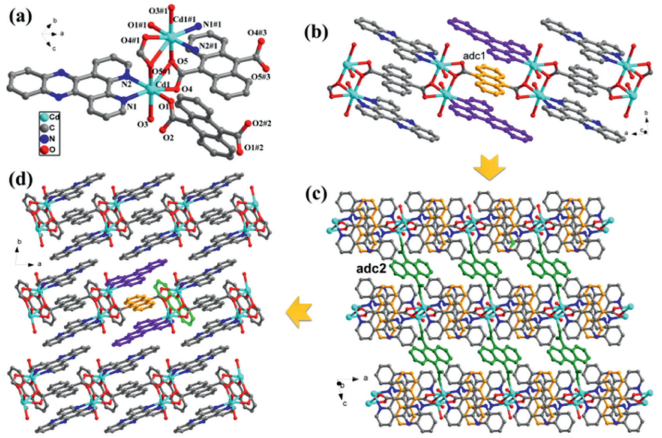


Fig. 2. Structures of DZU-401: (a) Coordination environment of the Cd centers. (b) The D−A chain structures formed by the connection of adc1 ligands with the Cd2 clusters. (c) The 2D layer structures formed by the connection of adc2 ligands with the D−A chains. (d) Packing mode of the final structures.

Structural analysis reveals that DZU-401 crystallized in the *P*-1 space group of the triclinic crystal system, with one Cd^{2+} ion center, one dppz ligand, one adc^{2-} ligand, and one coordinated water molecule in the asymmetric unit. As shown in Fig. 2a, Cd1 is bonded in a seven-coordinated manner with two nitrogen atoms from one dppz ligand, four carboxylic oxygen atoms from three adc^{2-} ligands, and one water molecule, to form a pentagonal bipyramid configuration. Similarly, binuclear $Cd_2(COO)_2(H_2O)_2$ clusters are also formed, which are further connected by the adc^{2-} ligands in a μ_2-η^2:η^1 mode (Fig. 2b, adc1) generating a 1D chain structure. Each anthracene unit of adc1 in the chains is parallelly encapsulated by two chelated dppz ligands to form the D−A chain structures, presenting the same D−A faces distance of 3.4 Å with DZU-400. Meanwhile, adc^{2-} ligands in η^1 modes as a linker (Fig. 2c, adc2) connect the D−A chain structures to form 2D layer structures. Neighboring layers then packed together and form the final supramolecular structures (Fig. 2d).

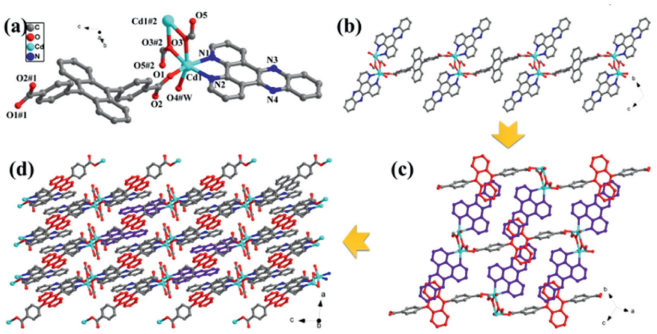


Fig. 3. Structures of DZU-402: (a) Coordination environment of the Cd centers. (b) The 1D chain structures formed by the connection of adb^{2-} ligands with the Cd2 clusters. (c) The D–A overlaps formed through the packing of adjacent 1D chains. (d) Packing mode of the final structures.

DZU-402 also crystallizes in the *P*-1 space group of the triclinic crystal system. Its asymmetric unit contains one Cd^{2+} ion, one dppz ligand, one-half of adb^{2-} ligand, one water molecule and one in-situ formed formate anion. Each Cd^{2+} ion coordinates with two nitrogen atoms from one dppz ligand, one oxygen atom from an adb^{2-} ligand, two oxygen atoms from two formate ligands, and one water molecule, to form an octahedral geometric configuration (Fig. 3a). Every two neighboring Cd^{2+} ions are bonded together by two oxygen atoms from two formate groups, forming binuclear $Cd(HCOO)_2(H_2O)_2$ clusters that are further bridged through adb^{2-} ligands in the η^1 mode to generate 1D chain structures (Fig. 3b). Different from DZU-400/401, the anchored dppz ligands and anthracene units in the chains do not produce D–A face-to-face overlaps. As shown in Fig. 3c, the D–A unit overlaps occur through the packing of adjacent chain structures and the D–A planes are not parallel with a dihedral angle of 11.9° The parallel A – A plane distance is about 7.0 Å and the closest distance between the D–A plane is 3.0 Å Finally, the chain structures stack and arrange in different directions through intermolecular force to form a 3D supramolecular structure (Fig. 3d).

As shown in Fig. 4, the planar chromophore (naphthalene, anthracene, anthracene) of the donor ligands (H_2ndc, H_2adc, H_2adb) in these DACPs is well restricted and dispersed in the acceptor dppz ligands. This means that the aggregation-caused quenching (ACQ) could be effectively avoided among the chromophores. Importantly, the proper distances (about 3.5 Å) and overlaps between donor and acceptor ligands could also enhance the D–A interactions, which is beneficial for the through-space charge transfer (TSCT) emission. Furthermore, the D–A interactions lead to different packing modes of the DACPs. In the step-like D–A chain structure of DZU-400, since each naphthalene just has large overlap with one adjacent dppz, there only exist discrete D–A unit stacking within each single chain, and the whole structure is further formed by $\pi\cdots\pi$ interaction of the dppz ligands from different chains (Figs. 4a and b). However, in DZU-401, each anthracene from the adc1 ligand overlaps largely with two dppz ligands, and the face-to-face ADA arrangement in each layer is further connected through the $\pi\cdots\pi$ interaction of the dppz ligands from different layers to form the ···AADAAD··· packing mode (Figs. 4c and d). As for DZU-402, due to the interchain D–A interactions, each anthracene unit of adb^{2-} ligand is inserted into the space between two dppz ligands from two adjacent chains, and therefore, by using the six-membered ring on two sides, the anthracene unit also overlaps with two dppz ligands to form ···AADAAD··· packing mode (Figs. 4e and f). Nevertheless, the D–A planes of DZU-402 are not parallel arranged, which is different from DZU-401. Moreover, the backbone of the donor ligand could be further decorated with functional groups such as -F, -Br and so on, which could be utilized for the tuning of the D–A properties.

In order to confirm the phase purity and framework stability of the DACPs, PXRD and TGA experiments were performed. First, as shown in Fig. S3 (Supporting information), the PXRD patterns of as-synthesized samples for these compounds are basically in accordance with their simulated ones, indicating the phase purity of these DACPs. Second, TG analyses (Fig. S5 in Supporting information) reveal that DZU-400/401/402 can be stable before 270, 305 and 345 °C, respectively. In detail, the TGA curve of DZU-400 exhibits a weight loss of 3.1 % at 200 °C, attributed to the removal of coordinated water molecules (calculated as 2.9 %). DZU-401 displays a 3.1 % weight loss prior to 305 °C, also indicating the removal of coordinated water molecules (calculated as 2.7 %). DZU-402 reveals two distinct weight loss plateaus prior to decomposition: the first stage, with a 2.9 % weight loss, occurs before 230 °C, corresponding to the loss of coordinated water molecules (calculated as 2.7 %) and the second stage, from 230 °C to 345 °C, exhibits an 8.4 % weight loss, attributed to the departure of formic acid molecules (calculated as 6.8 %) from the structure. Third, as further proved by variable temperature PXRD curves (Fig. S6 in Supporting information), the framework of DZU-400/401/402 could keep good crystalline at least under 200 °C. After that, although the diffraction peaks changed, which might be caused by the departure of coordinated solvent molecules, the main peaks were still observed, indicating their good framework stability.

Given the unique donor-acceptor structure that might exhibit unique photoluminescence based on the TSCT interactions, photophysical properties were systematically studied for the D–A com-

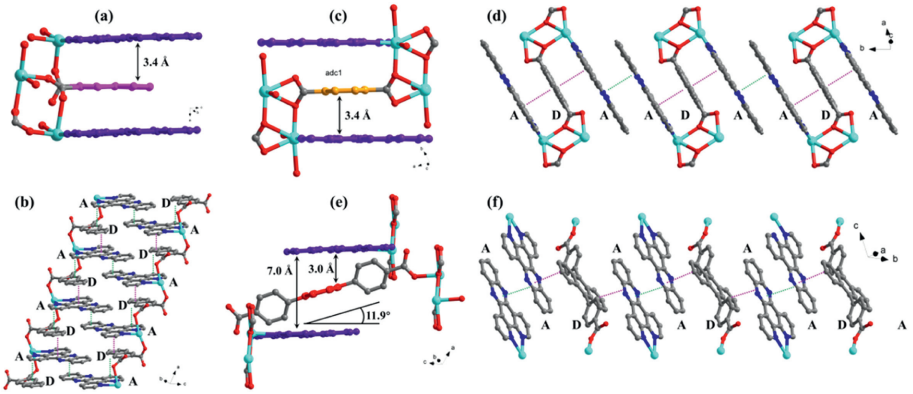


Fig. 4. Distances, overlaps and packing modes between donor and acceptor ligands in (a, b) DZU-400, (c, d) DZU-401, and (e, f) DZU-402. The purple dashed lines indicate the D–A interactions; the green dashed lines indicate the $\pi\cdots\pi$ interactions.

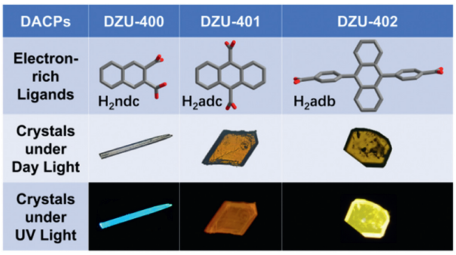


Fig. 5. Photographs of the DACPs with different donor ligands under daylight and UV light.

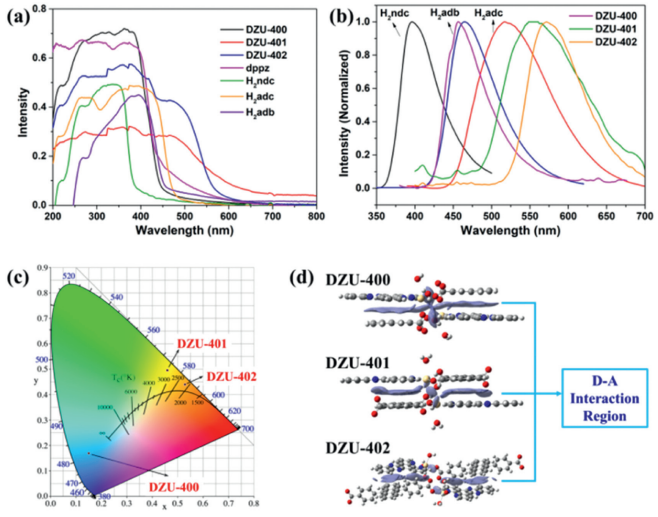


Fig. 6. (a) Solid state UV–vis spectra and (b) normalized fluorescence spectra of the DACPs and ligands. (c) The CIE coordinates of the DACPs. (d) Isosurface of δginter obtained from IGM analysis for the D−A interactions of the DACPs based on their crystal structures.

pounds. As shown in Fig. 5, the crystals of DZU-400, −401 and −402 are colourless, yellow, and orange under sunlight, respectively, which is consistent with their UV absorption spectra (Fig. 6a). While under UV light, blue, orange, and yellow emissions are observed, respectively. Subsequently, emission spectra of the compounds were tested under excitation of 365 nm. Fig. 6b reveals that the maximum emission peak are 457 nm for DZU-400, 555 nm for DZU-401 and 572 nm for DZU-402, respectively. The Commission Internationale de l'Eclairage CIE coordinates (Fig. 6c) were also calculated, which correspond well with their crystal colors and span a wide range from blue to orange. Notably, seen from the fluorescence comparison, the emissions are quite different from those of the luminescent donor ligands (H_2ndc: 396 nm; H_2adc: 517 nm; H_2adb: 465 nm) and reveal a varying degree of red shift. These emission behaviours should be originated from the TSCT between the different donor ligands and the acceptor dppz ligand. To verify this deduction, the interactions between D and A ligands of the DACPs were investigated with independent gradient model (IGM) analysis using Multiwfn software. Fig. 6d shows the isosurface of δ ginter with the lavender isosurface representing D−A interaction regions. Obvious isosurface distributions exist between the D and A ligands for all the DACPs, revealing the possibility of donor-acceptor charge transfer and thus the fluorescence emission characteristics based on donor-acceptor TSCT interactions.

The average fluorescence lifetimes (τ_{av}) and quantum yields (Φ_f) of the DZU-400/401/402 were also characterized (Fig. S7 in Supporting information and Table 1). The τ_{av} values were all in the nanosecond range, and among the three compounds, DZU-402 presents the highest τ_{av} value of 41.58 ns, with the highest Φ_f value of 3.98 %. All these results demonstrate that effective regulation of luminescent performance can be achieved in CPs by using different combinations of donor-acceptor ligands.

Table 1
Fluorescence data (λ_{ex} = 365 nm) of the DACPs.

DACP	λ_{em} (nm)	CIE	Φ_f (%)	τ_{av} (ns)
DZU-400	457	0.15,0.17	1.37	3.07
DZU-401	555	0.46,0.5	0.5	17.95
DZU-402	572	0.53,0.44	3.98	41.58
DZU-400-F	433	0.21,0.23	1.55	–-
DZU-400-Br	437	0.28,0.35	0.38	5280

Additionally, in this dppz based D−A system, we could not only achieve the successful construction of D−A materials with different photophysical properties through the tuning of the donor ligands, but also realize the precise modulation of luminescence based on the same D−A structure through ligand functionalization with different electronic characteristics. Taking DZU-400 as an example, Fig. S1 (Supporting information) reveals that after introducing -F or -Br atoms into the ndc^{2-} ligand, the obtained materials present similar framework structures with that of DZU-400, whereas their emission properties are different (Fig. S9 in Supporting information). DZU-400-F shows a main emission peak at 431 nm, while DZU-400-Br has two distinct peaks at 437 nm and 527 nm. Furthermore, the τ_{av} value of DZU-400-Br was significantly enhanced to 5.28 μs, compared to DZU-400. These results further demonstrate the high tunability of the DACP system obtained by strategy of combining ligand with planar A component and ligand with planar D component.

In order to further explore the potential applications of the DACPs, the emission spectra of the DZU-400, −401 and −402 were recorded from room temperature to 423 K. As shown in Figs. 7a-c, the intensity of the emission peaks for the three DACPs were reduced gradually in different degrees with the temperature increasing, which might be attributed to the gradual acceleration of the thermal motion of molecules. Notably, a pronounced blue shift in the emission spectrum was observed in DZU-402, which can be attributed to its distinct D−A interactions facilitated by the packing of adjacent chain structures. Specifically, one anthracene unit in each chain is found to overlap with two dppz ligands from the neighboring chains. This unique arrangement renders the D−A interactions more sensitive to temperature variations (Figs. S10 and S11 in Supporting information), which in turn accounts for the more pronounced temperature-induced emission shifts observed in DZU-402, compared to DZU-400 and DZU-401, in which the D and A units are face to face stacked in each single chain and stabilized by the coordination bonds. Then, the curves of fluorescence intensity with temperature were further plotted and fitted for the three DACPs to confirm the relationship between the emission intensity and temperature (Figs. 7d-f). It showed that the luminescence intensity of the DACPs all present good linear relationships under high temperature ranges (298–473 K), especially for DZU-400 which has an equation of $y = -0.0053x + 2.5703$ with $R^2 = 0.9982$. Moreover, the reversibility and repeatability of the DACPs were also determined (Figs. 7g-i and Fig. S12 in Supporting information), which reveal that the fluorescence intensity change is quite reversible with the temperature increasing/decreasing under high temperature range, and could be repeated at least three times without intensity change. Therefore, these temperature-dependent emission changes can be used for temperature sensing, demonstrating the potential as a fluorescence thermometer of these DACPs.

In summary, a new donor-acceptor coordination polymer system has been constructed through the combination of a phenazine based electron-deficient ligand and a series of aromatic-rings-

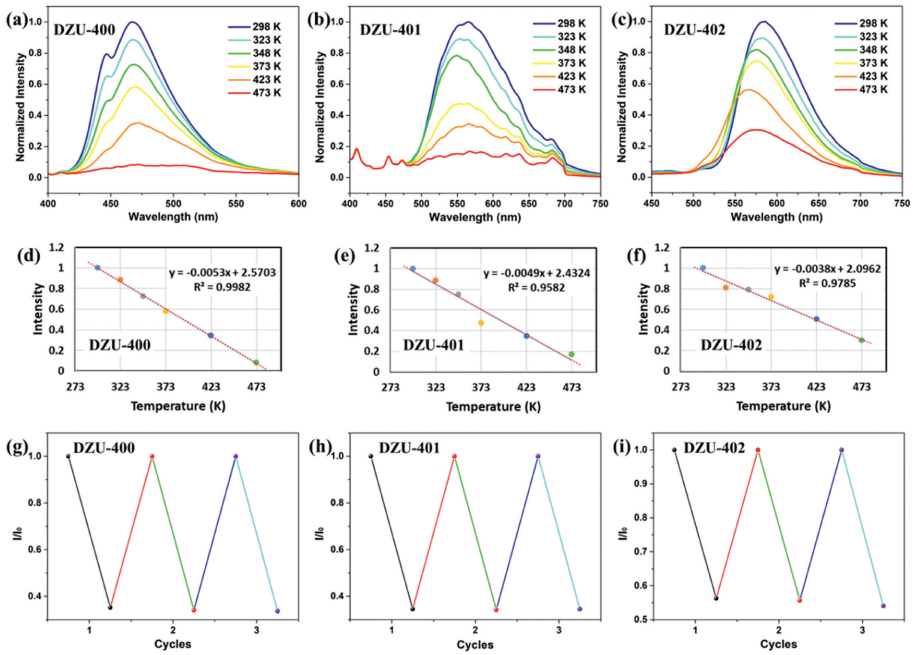


Fig. 7. Temperature sensing properties of the DACPs: (a-c) Various temperature fluorescence spectra. (d–f) The linear relationship between the emission intensity and temperature. (g–i) Cycling test of the temperature sensing for the DACPs.

based electron-rich ligands. The obtained DACPs show TSCT based luminescence, which could be regulated in a wide visible light range from blue to orange by modulating the donor ligands to tune the D−A overlaps. Moreover, the DACPs present high thermal framework stability, and show reversible and sensitive thermal-stimuli fluorescence responsive properties under high temperatures. This work may pave a way for the construction of new D−A materials with highly tunable luminescence and stimuli fluorescence responsive properties.

Declaration of competing interest

The authors declare that they have no known competing financial interests or personal relationships that could have appeared to influence the work reported in this paper.

CRediT authorship contribution statement

Zhen-Wei Zhang: Software, Methodology, Investigation, Data curation. **Da-Shuai Zhang:** Writing – review & editing, Writing – original draft, Funding acquisition, Conceptualization. **Wei Wang:** Investigation, Data curation. **Xiao-Ting Liu:** Writing – review & editing. **Hui Hu:** Methodology. **Yong-Zheng Zhang:** Methodology. **Longlong Geng:** Formal analysis. **Bin Li:** Formal analysis. **Yuchen Deng:** Formal analysis. **Rongmin Wei:** Methodology. **Xiuling Zhang:** Supervision. **Yuexing Zhang:** Writing – review & editing, Software. **Ze Chang:** Writing – review & editing, Conceptualization.

Acknowledgements

This work was supported by Qingchuang Talents Induction Program of Shandong Higher Education Institution, the National Natural Science Foundation of China (NSFC, Nos. 22405032, 22375104, 22201257, 21902022, 21601028), the Natural Science Foundation of Shandong Province (Nos. ZR2023QE104, ZR2022QE025, ZR2022QB058, ZR2021MB059, ZR2019QB026, ZR2018LB018), the Postdoctoral Fellowship Program of CPSF (No. GZC20232390) and Qingchuang Science and Technology Plan of Shandong Province (No. 2021KJ054).

Supplementary materials

Supplementary material associated with this article can be found, in the online version, at doi:10.1016/j.cclet.2024.110710.

References

[1] J. Zhang, W. Xu, P. Sheng, G. Zhao, D. Zhu, Acc. Chem. Res. 50 (2017) 1654–1662.
[2] X. Li, X. Kong, G. Sun, Y. Li, eScience 3 (2023) 100171.
[3] X. Wan, C. Li, M. Zhang, Y. Chen, Chem. Soc. Rev. 49 (2020) 2828–2842.
[4] L. Wang, W. Zhu, Adv. Sci. 11 (2024) 2307227.
[5] S. Izumi, H.F. Higginbotham, A. Nyga, et al., J. Am. Chem. Soc. 142 (2020) 1482–1491.
[6] Z. Chen, D. Zheng, R. Zhang, et al., Small Struct 4 (2023) 2300052.
[7] W. Tu, Z. Xiong, L. Wang, et al., Sci. China Chem. 67 (2024) 3121–3130.
[8] Q. Li, Y. Wu, J. Cao, et al., Angew. Chem. Int. Ed. 61 (2022) e202202381.
[9] X.F. Song, C. Jiang, N. Li, et al., Chem. Sci. 14 (2023) 12246–12254.
[10] J. Hu, Q. Li, X. Wang, et al., Angew. Chem. Int. Ed. 58 (2019) 8405–8409.
[11] S. Shao, L. Wang, Acta Polym. Sin. 53 (2022) 784–795.
[12] J. Wang, J. Miao, C. Jiang, et al., Adv. Opt. Mater. 10 (2022) 2201071.
[13] D.S. Zhang, Y.Z. Zhang, J. Gao, et al., Dalton Trans. 47 (2018) 14025–14032.
[14] X. Zhang, T. Li, J. Wei, et al., Dalton Trans. 51 (2022) 4790–4797.
[15] X. Zhang, R.H. Zhang, H. Hu, et al., Dalton Trans. 49 (2020) 2058–2062.
[16] X. Zhang, Y. Zhang, W. Zhou, et al., Chin. Chem. Lett. 34 (2023) 107368.
[17] D.S. Zhang, Z.W. Zhang, F.C. Li, et al., Inorg. Chem. 63 (2024) 15915–15923.
[18] Y.Z. Zhang, X.D. Zhang, Y.K. Zhang, et al., Inorg. Chem. Front. 11 (2024) 8101–8109.
[19] M. Boone, F. Artizzu, J. Goura, et al., Coord. Chem. Rev. 501 (2024) 215525.
[20] Q. Zhang, C. Huang, Y. Zhang, et al., Chem. Eng. J. 482 (2024) 148854.
[21] X. Li, K. Chen, R. Guo, Z. Wei, Chem. Rev. 123 (2023) 10432–10467.
[22] N. Hanikel, M.S. Prévot, O.M. Yaghi, Nat. Nanotechnol. 15 (2020) 348–355.
[23] A. Bigham, N. Islami, A. Khosravi, et al., Small 33 (2024) 2311903.
[24] R.E. Sikma, N. Katyal, S.K. Lee, et al., J. Am. Chem. Soc. 143 (2021) 13710–13720.
[25] T. Zhao, H. Wu, X. Wen, et al., Coord. Chem. Rev. 468 (2022) 214642.
[26] S. Yuan, J.S. Qin, J. Su, et al., Angew. Chem. Int. Ed. 57 (2018) 12578–12583.
[27] X. Shi, G.A. Lee, S. Liu, et al., Mater. Today 65 (2023) 207–226.
[28] C.Y. Lee, O.K. Farha, B.J. Hong, et al., J. Am. Chem. Soc. 133 (2011) 15858–15861.
[29] S. Mauree, V. Villemot, M. Hamel, et al., Adv. Funct. Mater. 33 (2023) 2302877.
[30] Y. Zhao, Y. Zhang, X. Cao, J. Li, X. Hou, Chem. Eng. J. 465 (2023) 143000.
[31] S.E. Gilson, M. Fairley, P. Julien, et al., J. Am. Chem. Soc. 142 (2020) 13299–13304.
[32] X.Y. Ren, F.Y. Chen, C.H. Zhang, et al., Chem. Eur. J. 30 (2024) e202402581.
[33] D.S. Zhang, Q. Gao, Z. Chang, et al., Adv. Mater. 30 (2018) 1804715.
[34] X.T. Liu, K. Wang, Z. Chang, et al., Angew. Chem. Int. Ed. 58 (2019) 13997 13997.
[35] X.T. Liu, W. Hua, H.X. Nie, et al., Natl. Sci. Rev. 9 (2021) nwab222.
[36] X.T. Liu, B.B. Qian, T. Zhang, et al., Matter 5 (2022) 2918–2932.
[37] B. Zhang, J. Xu, C.T. Li, et al., Angew. Chem. Int. Ed. 62 (2023) e202303262.
[38] K. Prasad, D. Samanta, R. Haldar, T.K. Maji, Inorg. Chem. 57 (2018) 2953–2956.